Research Square

Preprints are preliminary reports that have not undergone peer review.
They should not be considered conclusive, used to inform clinical practice,
or referenced by the media as validated information.

Carbon Nanotube Composites: Synthesis, Characterization, and Differential Antibacterial Activity Against S. aureus and E. coli

Qadoori Zedan Khalaf
Al-Iraqia University
kareem Al-Salihi
kareem.jibrael@univsul.edu.iq
University of Sulaymaniyah

Research Article

Keywords: Urea, Carbon nanotubes, Composite materials, Antibacterial activity

Posted Date: April 24th, 2026

DOI: https://doi.org/10.21203/rs.3.rs-9286958/v1

License: This work is licensed under a Creative Commons Attribution 4.0 International License.
Read Full License

Additional Declarations: No competing interests reported.

Carbon Nanotube Composites: Synthesis, Characterization, and Differential Antibacterial Activity Against S. aureus and E. coli

Qadoori Zedan Khalaf [a] Kareem Jumaah Jibrael Al-Salihi[b*]

[a]Department of Chemistry, College of Education, Al-Iraqia University, Baghdad, Iraq

E-mail: qadoorikhalaf1@yahoo.com

[b]*Department of Chemistry, College of Science, University of Sulaimani, Sulaymaniyah, Kurdistn region, Iraq,

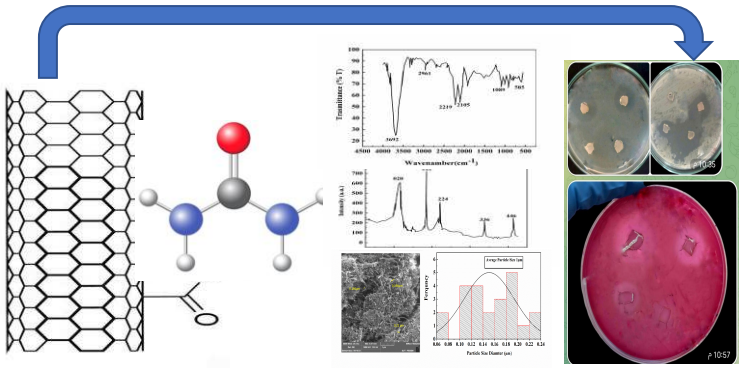
* Corresponding author: Kareem Jumaah Jibrael Al-Salihi E-Mail: kareem.jibrael@univsul.edu.iq

Abstract:

This study investigates the synthesis, characterization, and antibacterial evaluation of carbon nanotube (CNT) composites, with a focus on urea- and diamide-functionalized nanotubes. Amide nanotubes were synthesized through the self-assembly of amphiphilic molecules via hydrogen bonding, although scalability remains a challenge due to aggregation tendencies. Composites were prepared using varying weight ratios of urea or diamide with CNTs, and characterized using FTIR, XRD, SEM, and fluorescence microscopy to determine their structural and morphological properties. Antibacterial activity was assessed against Staphylococcus aureus and Escherichia coli using disk diffusion assays at concentrations of 50%, 75%, and 100% (w/v). Both composites, S1 (urea-CNT) and S2 (diamide-CNT), exhibited dose-dependent antibacterial effects, with S2 consistently showing larger inhibition zones than S1. The superior performance of S2 suggests enhanced antibacterial efficacy due to the diamide modification. These findings highlight the potential of amide-functionalized CNTs as effective antibacterial agents and support further development toward biomedical applications.

Keywords: Urea, Carbon nanotubes, Composite materials, Antibacterial activity.

Graphical Abstract



1. Introduction

Carbon nanotubes (CNTs) are considered one of the most promising nanomaterials due to their exceptional mechanical strength, high surface area, electrical conductivity, and chemical stability, making them suitable for a wide range of applications, including in nanomedicine and antimicrobial therapies [1,2]. However, pristine CNTs often exhibit limited solubility and biocompatibility, their biological properties are being studied in terms of toxicity [3]. Functionalization of CNTs, particularly through covalent and non-covalent modifications, is a widely employed strategy to overcome these limitations and improve their dispersion, stability, and targeted activity [3]. Among various functionalization approaches, amide-based modifications have attracted significant attention due to the strong hydrogen bonding capabilities and structural compatibility with biological molecules [4]. Amide linkages can be introduced onto the surface of CNTs through reactions with carboxyl or amine groups, allowing for the design of nanotube-based composites with improved bio-interactions and antibacterial activity [5].

The growing threat of bacterial resistance has intensified the search for novel antimicrobial materials with enhanced efficacy and biocompatibility [6]. Among the various nanomaterials explored, carbon nanotubes (CNTs) have garnered significant attention due to their unique structural, electrical, and mechanical properties, as well as their potential for functional modification [7, 8]. Surface engineering of CNTs with bioactive molecules can significantly

improve their interaction with microbial cells, thereby enhancing their antibacterial capabilities [8]. Amide-based functionalization, particularly with urea and diamide groups, offers a promising strategy for modifying CNTs through hydrogen bonding and self-assembly mechanisms, leading to well-defined nanotubular structures [9]. However, challenges such as aggregation and limited scalability remain barriers to their widespread application. These functionalized CNTs can interact with bacterial cell membranes, potentially leading to membrane disruption, oxidative stress, and cell death, especially in pathogenic bacteria such as Staphylococcus aureus and Escherichia coli [10]. Modifying the physicochemical properties of carbon nanotubes (CNTs) has been shown to significantly influence their cytotoxic effects in bacterial systems [11]. These findings highlight the importance of accurately documenting both physical and chemical characteristics when assessing the toxicity of carbon-based nanomaterials [12]. Studies have revealed that all CNT variants exhibit notable antimicrobial activity, although they differ in their capacity to induce oxidative stress and reduce colony-forming units across various microbial species [13]. Several parameters affect the antibacterial efficacy of CNTs, including their size (diameter and length), degree of aggregation, surface functionality, concentration, buffer environment, exposure time and intensity, and the specific bacterial strain involved [14].

Furthermore, nanocomposites such as reduced graphene oxide–silver nanoparticles (rGO–nAg) have demonstrated antibacterial effectiveness comparable to the systemic antibiotic nitrofurantoin against Proteus mirabilis and Staphylococcus aureus, and notably greater activity against Escherichia coli. The rGO–nAg nanocomposite exhibited faster bacterial inhibition than nitrofurantoin, likely due to the combined effects of membrane disruption through direct contact and oxidative stress. This finding contributes to a deeper understanding of the antibacterial mechanisms of rGO–nAg and can guide the development of graphene-based antimicrobial materials [15].

In another study, monodispersed, water-soluble, fluorescent carbon nanoparticles (CNPs) were synthesized from glucose via a one-step ultrasonic treatment with acid or alkali assistance. These CNPs featured surfaces enriched with hydroxyl groups, enhancing their hydrophilic nature [16].

The antibacterial performance of TiO_2/poly(lactic-co-glycolic acid) (TiO_2/PLGA) composites was evaluated against S. aureus and E. coli. In vitro wound healing studies using human keratinocytes (HaCaTs), fibroblasts (L929s), and bovine endothelial cells (BECs) seeded on TiO_2/PLGA

biofilms demonstrated that composites containing 10% TiO_2 nanoparticles offered significant antibacterial effects while maintaining cell viability and biocompatibility, suggesting their potential for safe tissue implantation [17]. Graphene has emerged as a promising green antibacterial agent, with broad-spectrum activity, minimal bacterial resistance, and acceptable cytotoxicity toward mammalian cells. Its antimicrobial action is driven by both mechanical and chemical mechanisms—physically disrupting bacterial membranes with its sharp edges and chemically inducing oxidative stress via reactive oxygen species and electron transfer. Moreover, graphene serves as an excellent platform to anchor metals, metal oxides, and polymers, enhancing antibacterial performance through synergistic effects [18]. Finally, functionalized multi-walled carbon nanotubes (F-MWNTs) have been studied as potential alternatives to conventional antibiotics. Their antimicrobial activity was tested against E. coli and S. aureus, revealing that the most effective concentrations for bacterial inhibition were 80 μg/mL and 60 μg/mL, respectively [19]. This study investigates the synthesis, structural characterization, and antibacterial performance of CNT composites functionalized with urea and diamide molecules. By evaluating their physicochemical properties and bactericidal activity against Staphylococcus and Escherichia coli, this research aims to identify the more effective composite and assess its suitability for potential biomedical use. The comparative analysis of these amide-functionalized CNTs contributes to the ongoing development of advanced nanomaterials for antimicrobial applications.

2. Experimental part

2.1 Chemicals and materials

Carbon nanotube, multi-walled, carboxylic acid functionalized (extent of labeling: >8% carboxylic acid functionalized) pursued from Sigma -Alde rich, Urea (purity 99.5%) was pursued from VWR Chemicals. Staphylococcus and Escherichia coli were (purity Greater than 85%) pursued from CUSABIO Technology LLC.

2.2 Synthesis of amide nanotubes (S1)

This procedure was adapted from the method described by Saeed et al. [20], in which 1 gram of urea and dissolve it in 20 milliliters of ethanol while stirring to ensure complete dissolution. Followed by adding an equal amount (1 gram) of wrapped carbon nanotubes to the urea-ethanol

solution. The reaction mixture is heated with continuous stirring under reflux for two hours to promote homogeneity and help the reaction between urea and carbon nanotubes. The produced precipitate has been filtered then washed with ethanol to eliminate any unreacted substances or impurities. Finally, the purified product is dried at 60°C to remove residual ethanol and obtain the final amide derivative.

2.3 Synthesis of diamide nanotube (S2)

Dissolve 0.5 g of compound (S1) in 20 ml of ethanol, then add 1 g of carbon nanotube. Heat the mixture under reflux for two hours. After completion, collect the resulting product and dry it at 60°C.

2.4 Biological activity test

The disk diffusion method is widely recognized as the gold standard for evaluating bacterial susceptibility to antimicrobial agents. This standardized approach was developed by Bauer and Kirby in 1956, following extensive optimization through the adjustment of various physical parameters [21]. In this technique, in this method, the isolated bacterial colony is selected, suspended into growth media, and standardized through a turbidity test [22]. Begin by dispersing the functionalized nanotube samples (S1 and S2) along with the non-functionalized control nanotubes in distilled water using ultrasonication for 30 to 60 minutes. Prepare suspensions at three different concentrations: 50%, 75%, and 100% weight/volume (w/v). Prepare bacterial suspensions of Staphylococcus aureus and Escherichia coli in saline solution, adjusting the turbidity to match a 0.5 McFarland standard. Using a sterile swab, evenly spread 100 µL of each bacterial suspension onto separate agar plates. Place sterile paper discs onto the agar surface. Then, carefully pipette 10 to 20 µL of each nanotube suspension onto individual discs. For comparison, include discs loaded with standard antibiotics as positive controls, and discs with only the solvent as negative controls. Incubate all plates at 37°C for 18 to 24 hours. After incubation, assess the plates for zones of inhibition and identify the Minimum Inhibitory Concentration (MIC) as the lowest nanotube concentration that prevents visible bacterial growth.

2.5 Characterization methods

XRD

The XRD pattern was recorded using a Rigaku D/MAX-rA Xray diffractometer with Cu Ka radiation (δ = 0.15418 nm). The sample was scanned for 2Θ values ranging from 3º to 80º with a scan speed of 1/min.

FT-IR

FTIR spectrum was obtained using a Bruker Tensor 27 FT-IR Spectrometer where samples will be were finely ground and mixed with KBr and pressed into a disc. Spectrums of samples were scanned at 2 cm^{-1} resolution between 500 and 4000 cm^{-1}.

Scanning Electron Microscopy (SEM)

Scanning Electron Microscopy (SEM) was employed as a powerful method to analyze the surface morphology of a composite material made of urea supported on carbon nanotubes. To evaluate the effectiveness of the sorption process, SEM images of both composite materials are shown in Figures 7 and 8. As illustrated in the figure, hierarchical micro- and nanostructures developed, displaying various textural pores that became more prominent at higher magnifications. The morphology and particle size were influenced by the presence of cationic ions, which help minimize the surface energy disparity between polar and nonpolar crystal planes.

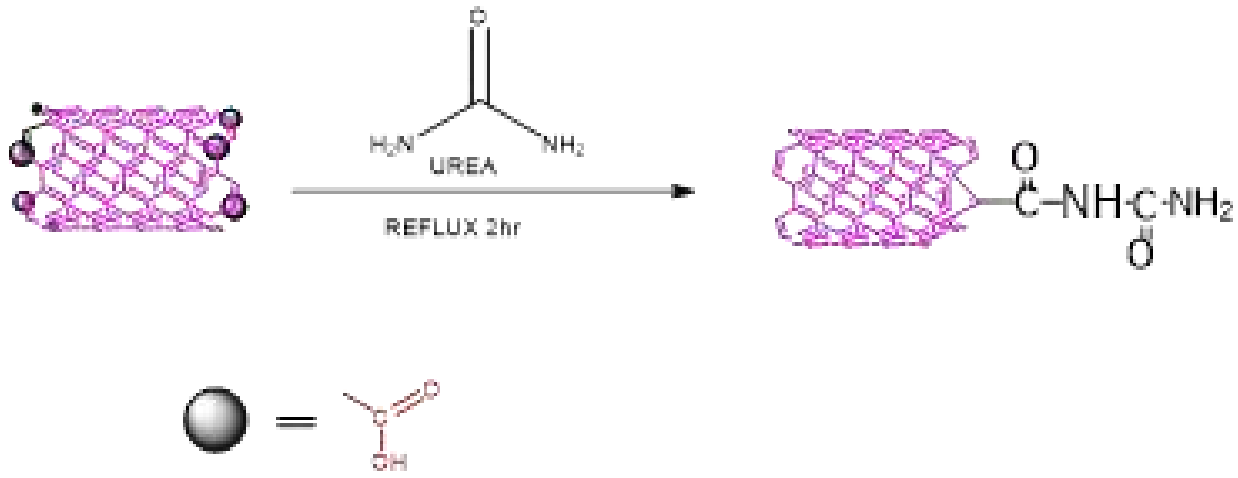
Atomic Force Microscopy (AFM)

The surface morphology and topographical features of the diamide carbon nanotube (CNT) composite were investigated using Atomic Force Microscopy (AFM) NT-MDT Prima, Bruker Dimension Edge, Bruker Dimension ICON, Agilent 5500. The measurements were performed in tapping mode using a high-resolution AFM instrument. Samples were prepared by depositing a dilute dispersion of the composite material onto freshly cleaved mica substrates, followed by drying under ambient conditions. The scan area was set to 11.6 μm × 11.6 μm, and images were captured in both forward and backward directions along the Z-axis using a line-fit processing mode to enhance feature resolution. Height and phase images were analyzed to evaluate surface roughness, particle distribution, and morphological anisotropy. The AFM images revealed elongated nanostructures and directional alignment of the diamide-functionalized CNTs, indicative of interactions between the organic diamide groups and the nanotube surfaces.

3. Results and discussion

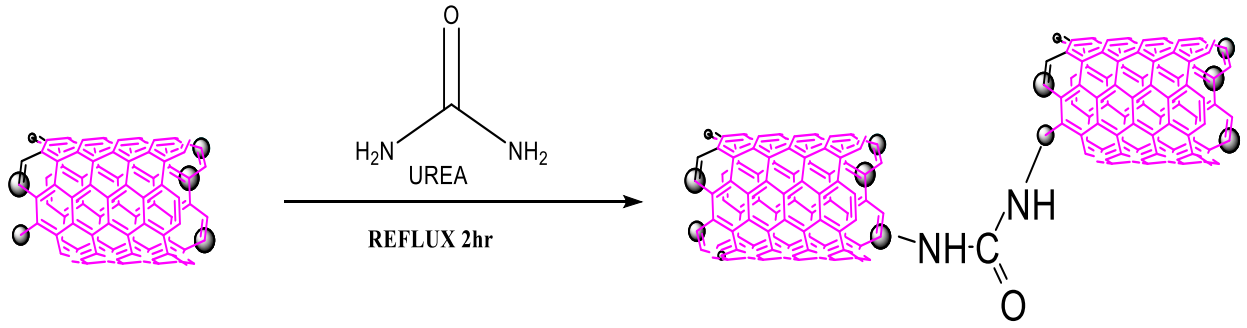
Amide nanotubes are typically synthesized through the self-assembly of amphiphilic molecules containing amide functional groups. These nanotubes are primarily formed through hydrogen bonding interactions, leading to well-defined tubular architectures [23].

The molar ratio of urea to carbon nanotubes is a key factor that influences the degree, effectiveness, and nature of the functionalization achieved on the CNT surface. Urea is often selected as a functionalizing agent because it can add amide or carbamoyl groups to the nanotubes through thermal or chemical processes, which enhances their dispersion, reactivity, and compatibility with polymer or composite materials [24]. When the mole ratio is appropriately balanced, the majority of urea molecules interact with only a single reactive site on the CNT surface or defect area. This condition generally results in mono-amide functionalization as shown in scheme 1. where one amide group attaches to the nanotube while the other potential reactive groups stay unreacted or undergo rearrangement.



Scheme1: Chemical reaction step of mono-amid nanotube preparation (S1).

When the number of reactive CNT sites exceeds the amount of urea, each urea molecule typically attaches to only one site on the nanotube. Conversely, when urea is supplied in excess compared to the available CNT sites, the likelihood that both amine groups or reactive ends of the urea molecule participate in bonding increases as shown in the scheme 2. Under these conditions, di-amide functionalization is favored, allowing urea to connect two CNT sites and produce a more densely modified surface.



Scheme2: Chemical reaction steps of di-amide nanotube preparation (S2).

However, their synthesis can be more challenging due to increased aggregation tendencies, requiring precise experimental conditions. The scalability of these nanotubes remains a challenge, and optimizing synthesis for large-scale production is an ongoing research focus.

3.1 XRD Analysis of Urea/CNT Composite

The crystallinity and layered structural properties of the starting materials and the amide carbon nanotubes were examined using X-ray powder diffraction (XRD). The corresponding results are illustrated in Figure 1 shows the X-ray diffraction (XRD) pattern of carbon nanotubes (CNTs)

The reflection peaks were identified at approximately 2θ = 26°, 43°, 50°, and 77°, which align with the (002), (100), (101), and (006) crystallographic planes, respectively [24]. The Peak at 26° (2θ) Indexed as (002) is the most intense and sharp peak, indicating a high degree of graphitization. This corresponds to the interlayer spacing of graphite-like structures (3.4 Å), characteristic of the graphitic walls in carbon nanotubes. A sharp and intense peak here implies well-ordered multi-walled CNTs with good crystalline nature in the stacking direction. Additional weaker peaks ((100), (101), and (006)) support the presence of a partially crystalline, hexagonal graphitic structure typical of multi-walled CNTs. Overall, the CNTs appear to be well-structured with some degree of crystallinity, common in high-quality synthesized carbon nanotubes [25].

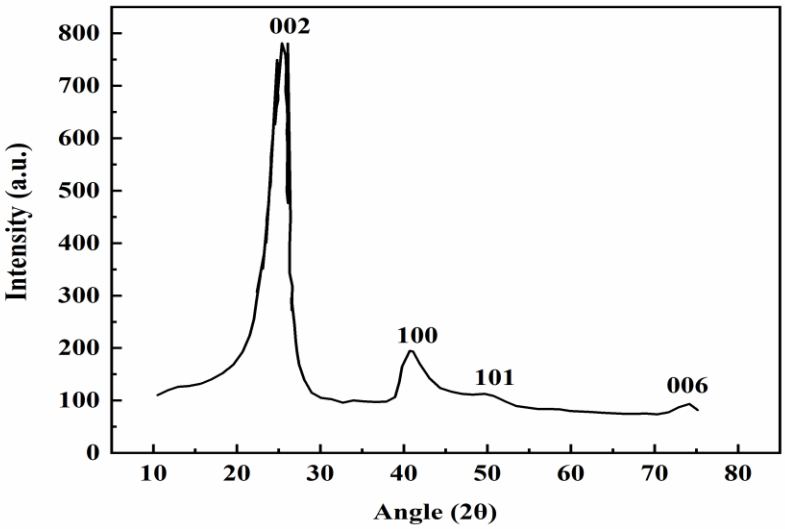


Figure 1: X-ray diffraction (XRD) pattern of carbon nanotubes (CNTs)

The XRD pattern displays sharp diffraction peaks at specific 2θ values, indicating that urea is present in a crystalline form. Figure 2. Shows the major peaks at 2θ = 22°, 35°, 58°, and 78°are indexed to the crystal planes (110), (210), (212), and (420), which are consistent with urea's known orthorhombic crystal system. The observed Peak at (2θ = 22º) indexed as (110) is the most intense peak, suggesting a preferred orientation or high crystallinity along the (110) plane [26]. The second peak at 35° (210) is a secondary high-intensity peak, indicating a prominent (210) reflection. The peak at (2θ = 58º) indexed as (212) supports the ordered structure of the urea crystal lattice. The peak at (2θ = 78º) indexed as (420) a higher-angle peak confirming the presence of fine periodicities in the crystal.

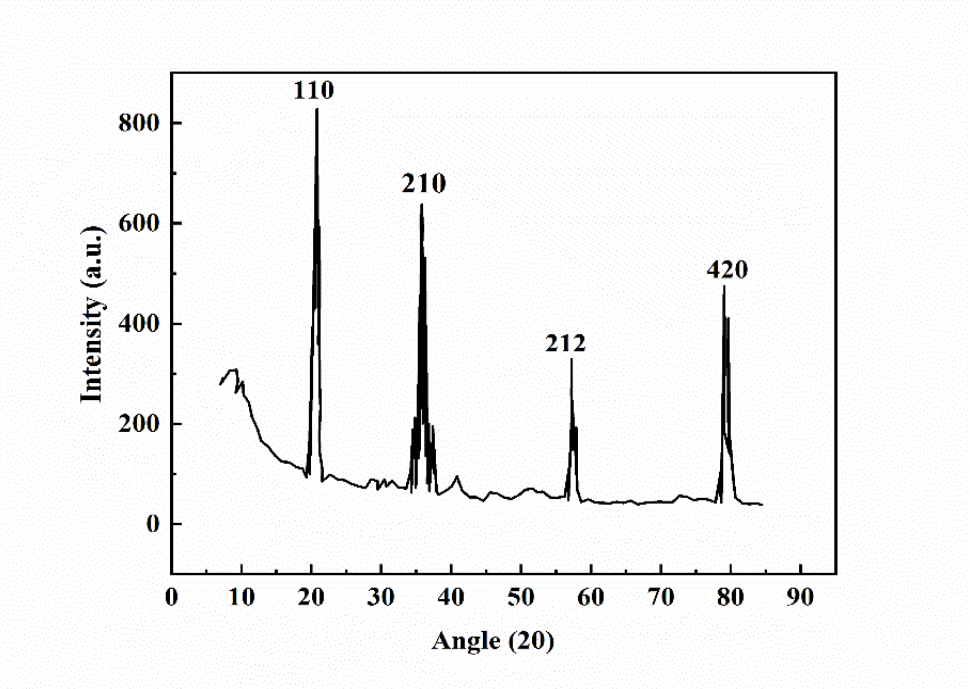


Figure 2: X-ray diffraction (XRD) pattern of urea.

Figure 3, shows the XRD (X-ray diffraction) pattern of the crystallographic features of a composite material made of urea supported on carbon nanotubes (CNTs). The peaks at specific 2θ values at 22°, 35°, 43°, 65° and 79° indicate the presence of crystalline phases in the composite. Labeled planes: (020), (222), (224), (336), and (446) respectively, reflect distinct crystal orientations, likely originating from urea in a well-crystallized form. The Peak at 20° (2θ) Indexed as (020) corresponds to urea, consistent with reported diffraction peaks in urea-based material. The most intense peak, suggesting that the (222) crystal plane is the dominant orientation. It indicates strong crystallinity and preferential growth of urea crystals on this plane [27].

The peaks at (224), (336), and (446) (2θ ≈ 43°, 65°, and 79°, respectively) also suggest highly ordered urea crystallites. CNTs usually show a broad peak near 2θ =22°, corresponding to the (002) plane of graphitic carbon. In this pattern, the CNT signature is either very weak or overshadowed by the strong peaks of urea. This indicates that urea dominates the crystalline structure, or that CNTs are present in a lower crystalline/amorphous state or low quantity.

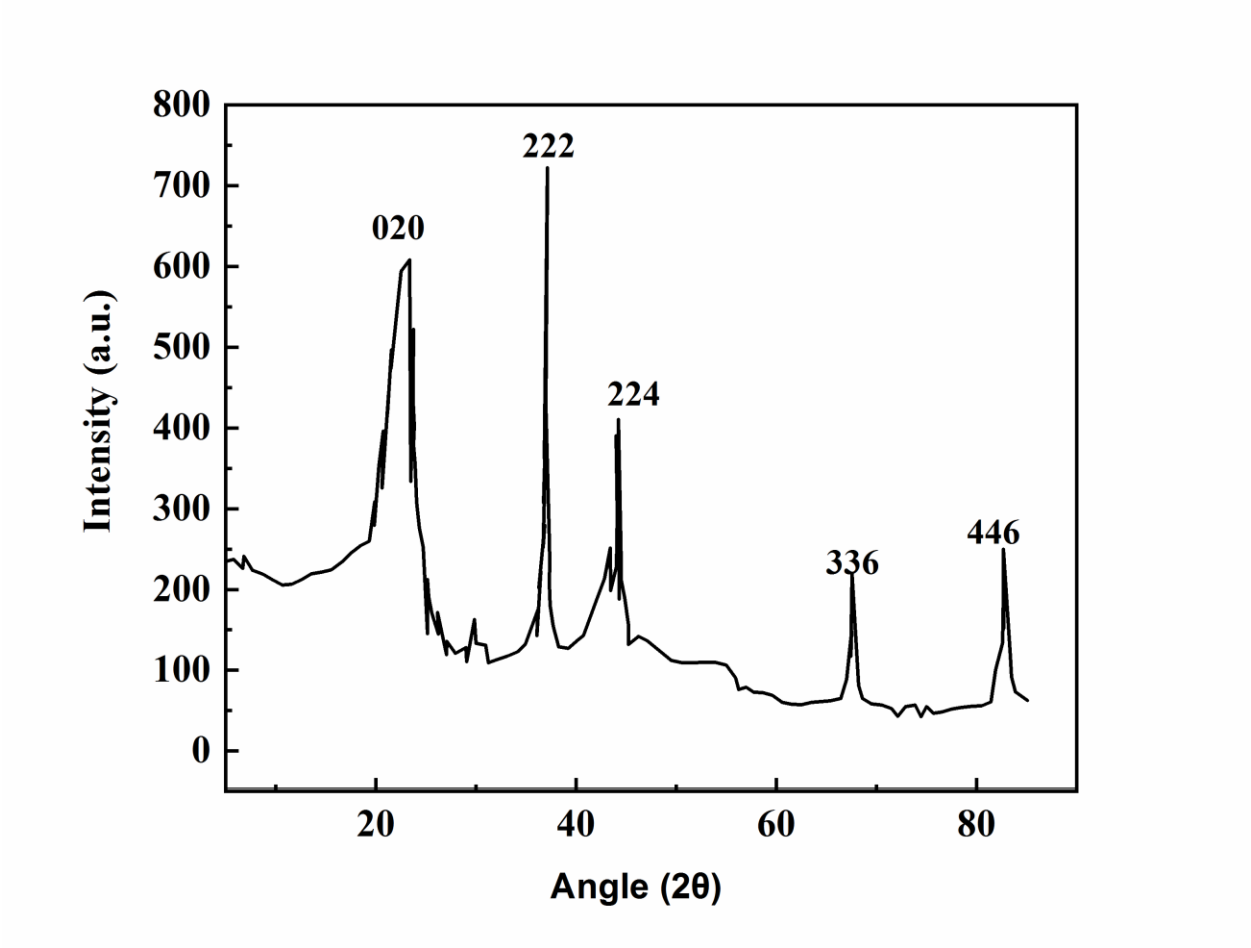


Figure 3: XRD (X-ray diffraction) pattern of a composite material made of urea supported on carbon nanotubes (CNTs).

The XRD pattern shown in the figure 4 represents the crystalline structure of a composite material composed of diamide and carbon nanotubes (S2). The broad peak at (2θ) 26° Indexed as (002) is characteristic of carbon nanotubes (CNTs) and corresponds to the (002) diffraction plane of graphitic carbon. The broadness indicates a semi-crystalline or amorphous nature, typical of CNTs with some structural disorder or smaller crystallite size [28]. The intense and sharp peak at (2θ) 27° indexed as (222) suggests the presence of a highly crystalline phase in the composite. This may be due to the diamide component, which has crystallized within or on the CNTs. The peaks

at 2θ (44.5°, 66.5°, and 78°) the systematic indexing (224, 336, 446) are sharp and well-defined, confirming the crystalline nature of the diamide compound [29]. That indicates a possible cubic or orthorhombic crystal structure of the diamide or a metal-organic framework derived from it.

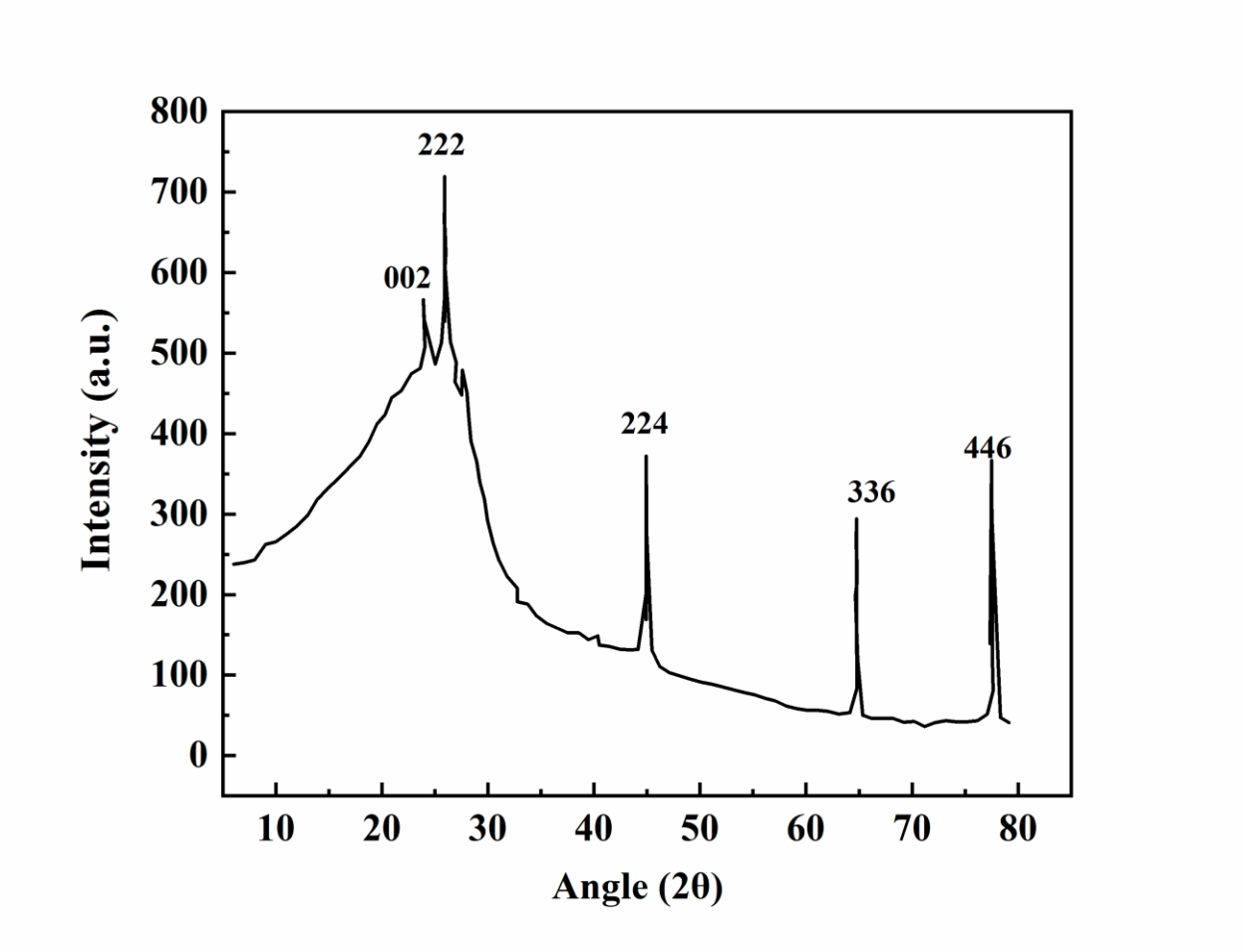


Figure 4: XRD (X-ray diffraction) pattern of a composite material of diamide carbon nanotubes (S2).

3.2 FT-IR Analysis of Urea/CNT Composite

Figure 5, shows the FT-IR (Fourier-transform infrared) spectrum of a urea composite on carbon nanotubes (CNTs). Doublet strong absorption peak between 3200–3600 cm^{-1} suggests N–H stretching (-NH_2 group) A strong absorption around 1700 cm^{-1} typically indicates a carbonyl group (C=O). The peaks 1450–1600 cm^{-1} due to N–H bending and C–N stretching (amide II band) [30]. These peaks are related to the amide functionality in urea and may shift when urea interacts with

CNTs. In addition, the peaks 1300–1000 cm^{-1} due to C–N stretching, C–O stretching Indicates the C–N bonds in urea and potential interactions with CNT functional groups (like carboxyl or hydroxyl). And the peaks 800–600 cm^{-1} is Out-of-plane bending modes. These may represent CNT backbone vibrations or interactions between CNT and urea. The FT-IR spectrum confirms the presence of urea functional groups (N–H, C=O, C–N) and indicates successful interaction or adsorption of urea onto carbon.

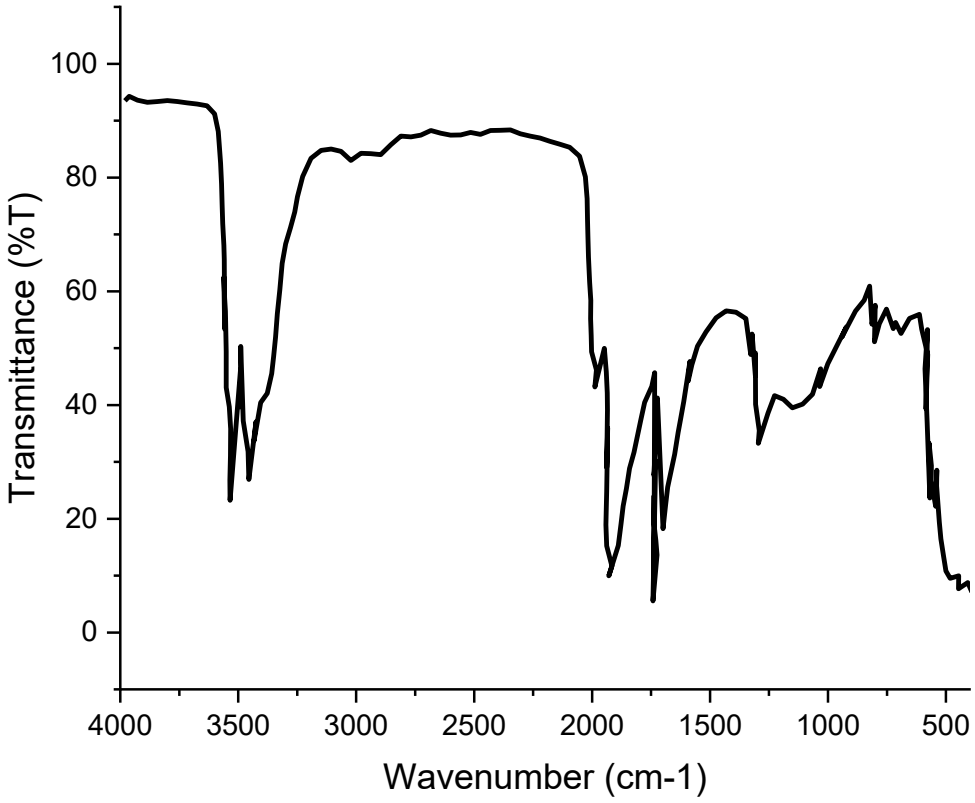


Figure 5: FT-IR spectrum of a composite material made of urea supported on carbon nanotubes (CNTs.

Figure 6 show the FT-IR spectrum the major peaks labeled of a diamide carbon nanotube (CNT) composite. The strong, sharp absorption band at 3692 cm^{-1} corresponds to the N–H stretching vibrations indicates the presence of amide N–H. The peak 2219 cm^{-1} associated with C–H stretching vibrations of alkyl groups. Suggests the presence of hydrocarbon chains or surface

functionalization with alkyl-containing diamide groups. The peaks at 2219 cm^{-1} and 2105 cm^{-1} indicate to aliphatic chains (C–H), and possibly nitrile/alkyne moieties, suggesting successful chemical bonding of diamide groups onto the carbon nanotube surface. The peak 1089 cm^{-1} typically assigned to C–N stretching or C–O stretching vibrations. Supports the presence of amide bonds, indicating successful functionalization of CNTs with diamide. The low-frequency region peaks 585 cm^{-1} is often attributed to metal–oxygen or C–C skeletal vibrations in CNTs. In this case, it may reflect the carbon nanotube backbone structure or bending modes of the CNTs functionalized with diamide [31].

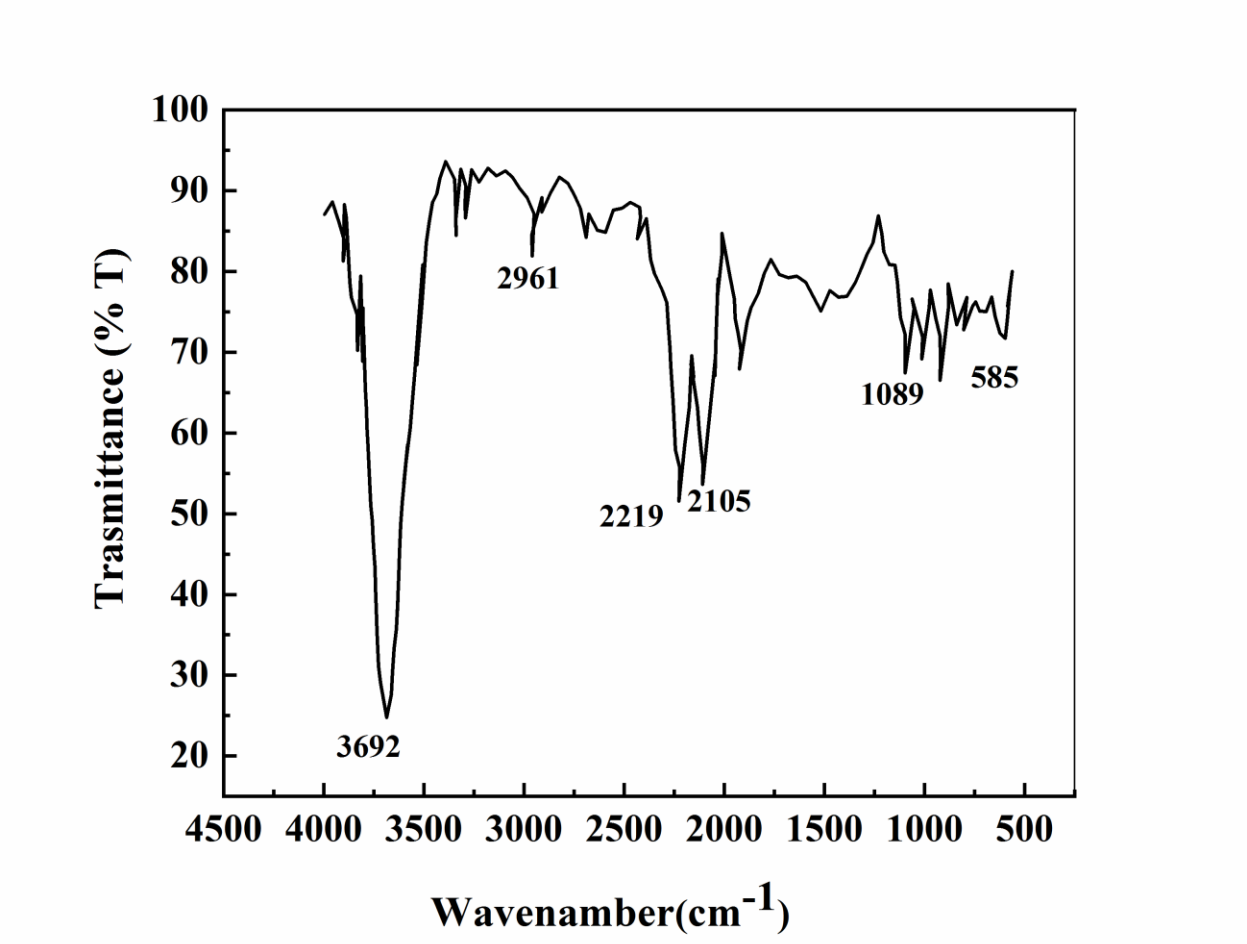


Figure 6: FT-IR spectrum of a composite material of diamide carbon nanotubes (S2).

3.3 SEM Analysis of Urea/CNT Composite

The surface morphology of the urea/CNT composite was investigated using scanning electron microscopy (SEM) as shown in figure 5. The SEM images revealed a network of entangled carbon nanotubes with diameters ranging from 20 to 40 nm, forming a porous, web-like structure. Upon loading with urea, the surface of the nanotubes appeared coated with irregular, granular particles. These particles, attributed to crystallized urea, were found to be unevenly distributed along the CNT surfaces. Compared to pristine CNTs, which exhibit smooth and clean surfaces, the urea-loaded CNTs demonstrated a rougher texture, indicating successful deposition of urea. At higher magnification, the urea particles appeared to partially agglomerate in localized regions, potentially due to hydrogen bonding and van der Waals interactions between urea molecules and the CNTs. No significant structural collapse or damage to the nanotube framework was observed, suggesting that the composite preparation preserved the CNT integrity [32]. These observations confirm the physical adsorption and successful incorporation of urea onto the CNT matrix, potentially enhancing the composite's surface reactivity and nitrogen content for applications such as controlled-release fertilizers or chemical sensing.

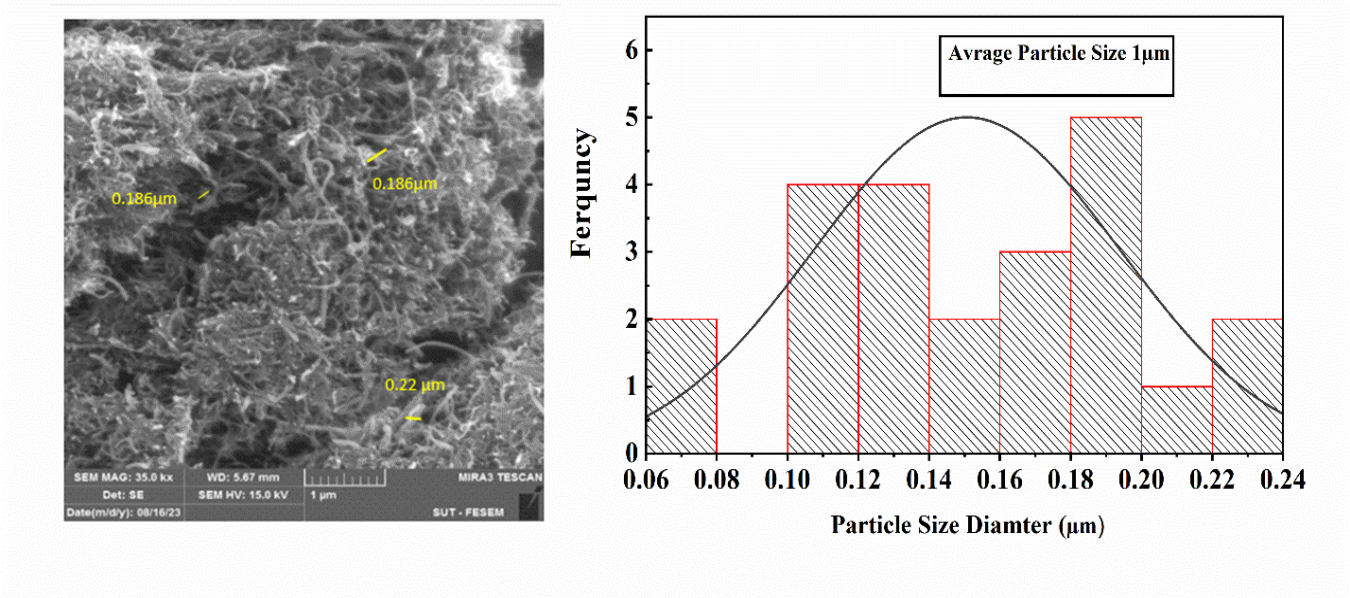


Figure 7: SEM image of a composite material made of urea supported on carbon nanotubes (CNTs).

3.4 AFM Analysis of Urea/CNT Composite

Figure 8 presents a Scanning Electron Microscopy (SEM) image and a particle size distribution histogram of a composite material composed of diamide supported on carbon nanotubes (CNTs). These measurements suggest a relatively nanoscale dispersion of urea particles on the CNT framework. The particles appear to be irregularly shaped and clustered, which is typical in composites formed via physical or chemical deposition. The carbon nanotube network likely forms the darker, fibrous background, while urea particles appear as brighter, roughly spherical or elliptical formations. The histogram shows the frequency distribution of particle sizes ranging from 0 to 500 nm. Indicating a relatively symmetric spread of particle sizes most particles fall within the 100–300 nm range. The SEM and particle size analysis together confirm nanoscale integration and dispersion, which are critical for the material's potential performance in catalysis, adsorption, or electronic applications.

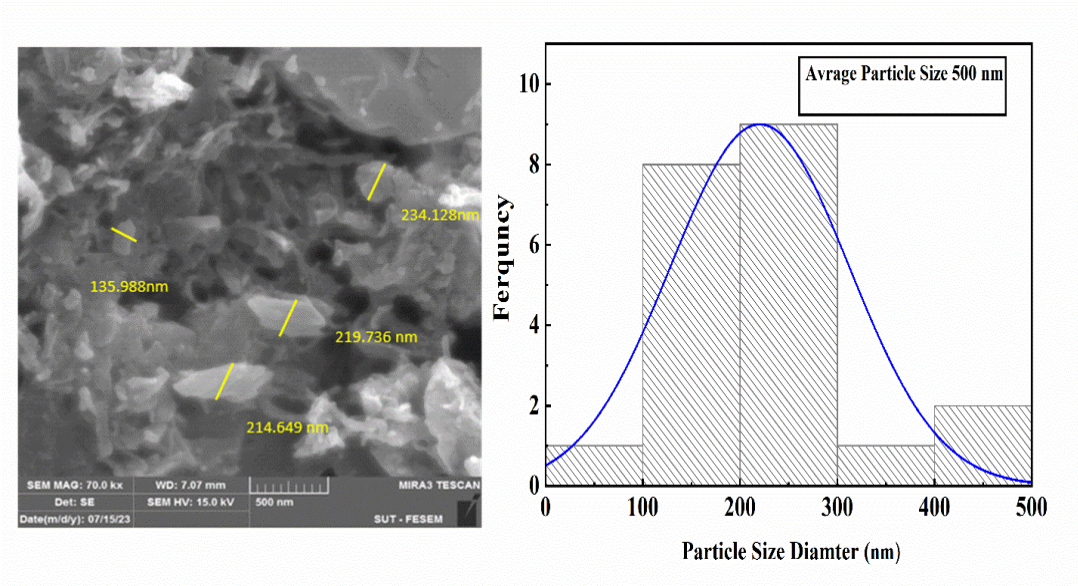


Figure 8: SEM image of a composite material of diamide carbon nanotubes (CNTs).

Figure 9, presents an Atomic Force Microscopy (AFM) image illustrating the surface topography of a urea–carbon nanotube (CNT) composite, acquired using a scan size of 11.6 µm × 11.6 µm in Z-Axis – scan forward – line fit mode. The image displays a distinct anisotropic pattern characterized by diagonally oriented, elongated bright regions. These elevated features correspond to areas with greater height, suggesting the presence of urea particles or aggregates deposited across the CNT surface. The dimmer, more continuous background with a smoother texture likely

represents the underlying CNT network, which is known for its fibrous, cylindrical morphology. In AFM imaging, CNTs generally appear as fine raised lines or bundles unless significantly coated.

The sharp and bright streaks indicate the formation of urea crystallites or clusters anchored onto the nanotubes [33]. The variation in size and irregular distribution of these features' points to partial surface coverage and non-uniform nucleation, implying a heterogeneous deposition process. Overall, the AFM analysis verifies the successful incorporation of urea onto the CNT framework, showing nanoscale interaction and attachment, which may suggest potential interfacial bonding or adhesion between the two components.

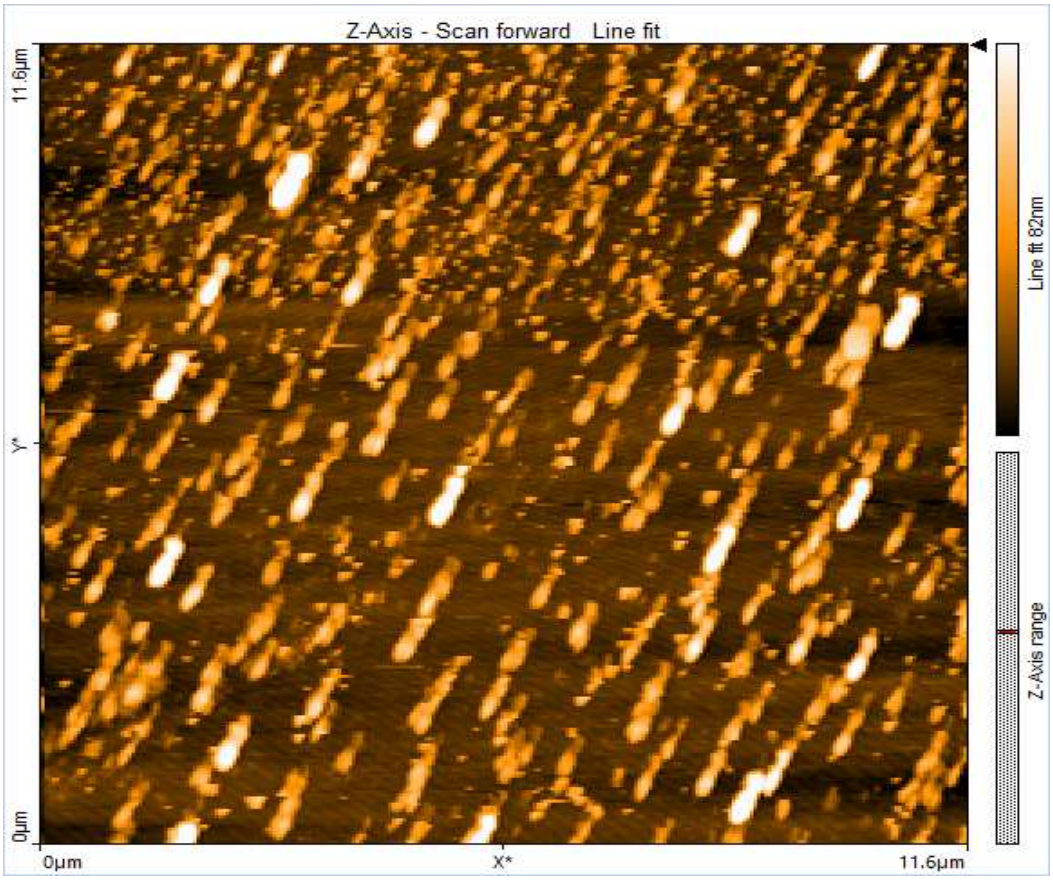


Figure 9: AFM image of a composite material made of urea supported on carbon nanotubes.

The AFM image in figure 10, illustrates the surface topography of a composite material consisting of diamide-functionalized carbon nanotubes. The image displays elongated, fibrous structures distributed across the scanned surface, which are characteristic of carbon nanotube morphology.

These nanotubes appear more interconnected and sometimes bundled, suggesting cross-linking or aggregation, potentially due to diamide interaction. The presence of non-uniform thickness or granular decorations on the nanotubes suggests successful diamide functionalization, which can cause increased height variation.

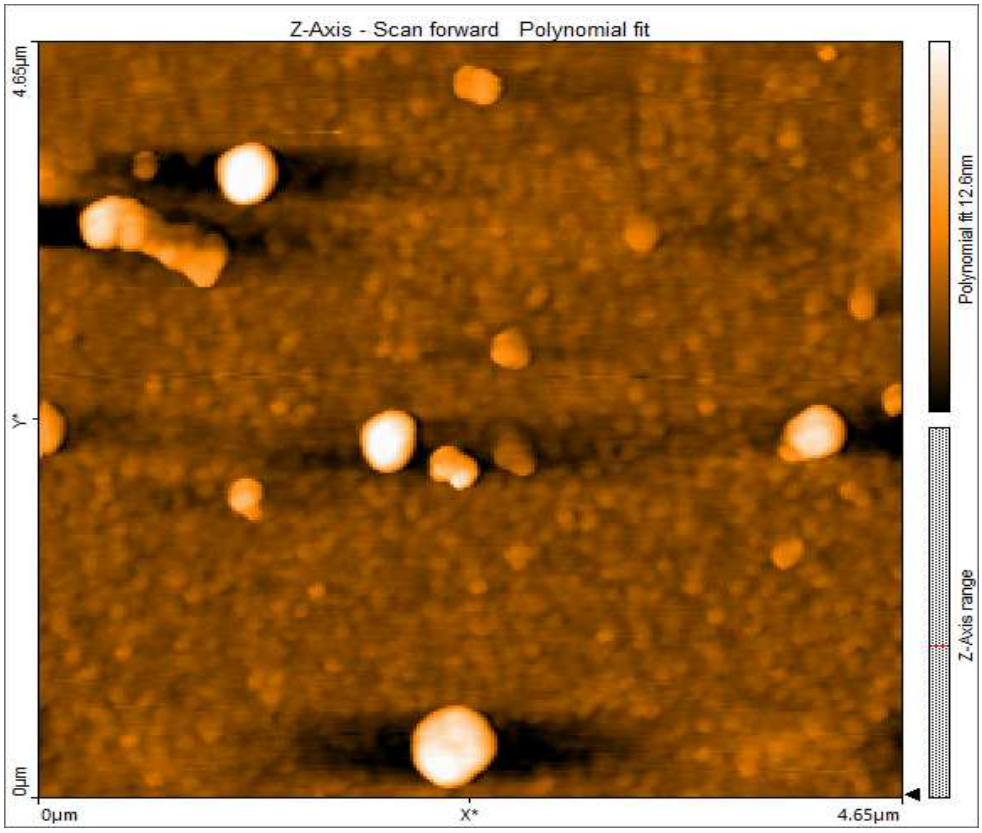


Figure 10: AFM image of a composite material of diamide carbon nanotubes.

3.5 Biological activity of the prepared compounds

The synthesized composite compounds from urea supported on carbon nanotubes demonstrated inhibitory effects against certain bacterial species of Staphylococcus and Escherichia coli with activity levels depending on the concentration used higher concentrations corresponded to greater antibacterial action. The functionalized carbon nanotube samples (named as S1 and S2) and the non-functionalized control nanotubes were individually dispersed in distilled water. Separately, bacterial suspensions of *Staphylococcus aureus* and *Escherichia coli* were prepared in sterile saline solution to be used for subsequent antimicrobial have been tested as shown in figure 11. The

dispersions were subjected to ultrasonication for a duration of 30 to 60 minutes to ensure uniform distribution. Three distinct weight/volume (w/v) concentrations were prepared for each sample (50%, 75%, and 100%).

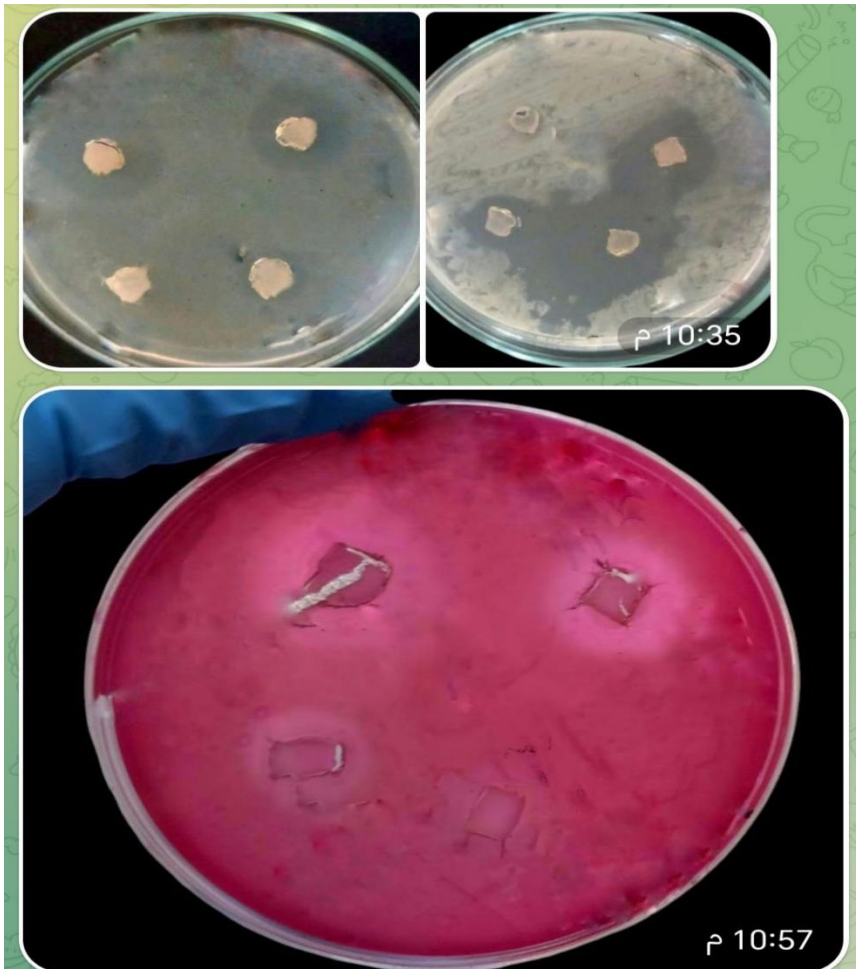


Figure 11: Preparation bacterial suspensions of Staphylococcus and Escherichia coli in saline solution.

The antibacterial performance of the compounds at different concentrations (100%, 75%, and 50% w/v) of the synthesized composite compounds from urea supported on carbon nanotubes demonstrated inhibitory effects against certain bacterial species of Staphylococcus were measured by the diameter of the inhibition zones (in mm) and the data have been listed in Table 1.

Table 1: Inhibition circle width of a composite of urea on carbon nanotubes (S1) and composite diamide on carbon nanotube (S2) against Staphylococcus.

Compound	100%	75%	50%
S1	25	20	12
S2	30	22	8

The histogram in figure 12 shows the antibacterial activity of two samples named S1 and S2 which prepared from urea sported on carbon nanotubes Staphylococcus bacteria at three concentrations (50%, 75%, and 100%). For both composite materials S1 and S2, the inhibition zone increases as concentration increases from 50% to 100%, indicating a dose-dependent antibacterial effect. At each concentration (50%, 75%, and 100%), the compound S2 shows larger inhibition zones than S1, which suggests that the urea-CNT composite is more effective in inhibiting Staphylococcus growth compared to the individual components. The composite of urea supported on carbon nanotubes enhances antibacterial activity against Staphylococcus, it might be due to the synergistic effect of carbon nanotubes which may disrupt bacterial membranes and urea which may exert chemical stress on the bacteria.

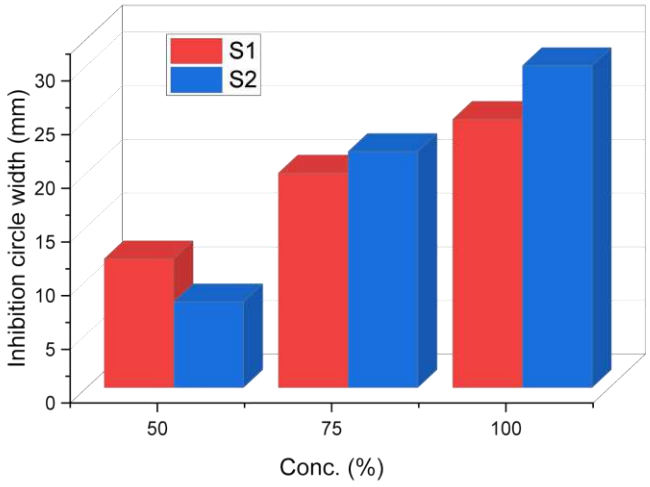


Figure 12: Histogram Inhibition circle width of a composite of urea on carbon nanotubes (S1) and composite diamide on carbon nanotube (S2) against Staphylococcus.

The antibacterial performance of the compounds S1 and S2 at different concentrations (100%, 75%, and 50% w/v) of the synthesized composite compounds from urea supported on carbon nanotubes demonstrated inhibitory effects against certain bacterial species of Escherichia coli were measured by the diameter of the inhibition zones (in mm) and the data have been listed in Table 2.

Table 2: The data of inhibition circle width of a composite material of urea on carbon nanotubes against Escherichia coli.

Compound	100%	75%	50%
S1	23	22	9
S2	33	28	12

Figure 13, histogram illustrates the antibacterial effectiveness of two different composites S1 (urea on carbon nanotubes) and S2 (diamide on carbon nanotubes) against Escherichia coli, measured

by the inhibition circle width in millimeters (mm) at three different concentrations 50%, 75%, and 100%. The compound S2 (diamide-CNT) Slightly higher (13 mm), showing better antibacterial effect than compound S1 (urea on carbon nanotubes). The results show both composites dose-dependent antibacterial activity inhibition increases with concentration. And S2 (diamide-CNT) is more effective than S1 at all tested concentrations [34]. This suggests that the diamide modification enhances the antibacterial properties of carbon nanotubes more significantly than urea when targeting Escherichia coli.

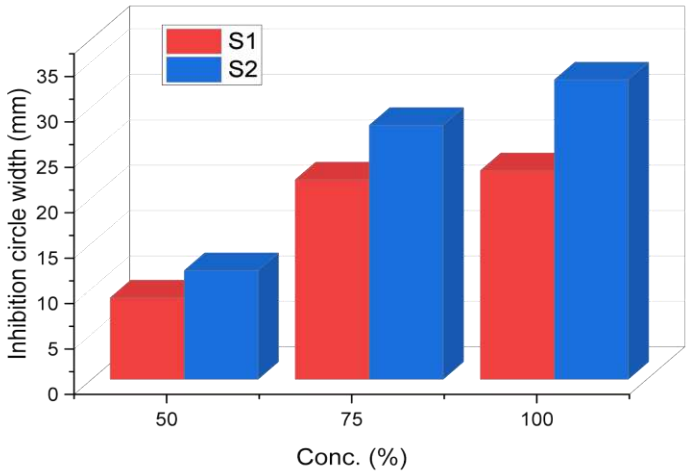


Figure 13: Histogram Inhibition circle width of a composite of urea on carbon nanotubes (S1) and composite diamide on carbon nanotube (S2) against Escherichia coli.

Conclusion

This study successfully demonstrated the synthesis and characterization of amide-based carbon nanotube composites using urea and diamide functionalization, aiming to enhance antibacterial performance. Structural and morphological analyses confirmed the formation of distinct nanocomposites, and biological assays revealed notable antibacterial activity against both Staphylococcus aureus and Escherichia coli. The results indicate that antibacterial efficacy is concentration-dependent, with higher concentrations yielding larger inhibition zones. Notably, the diamide-functionalized composite (S2) consistently outperformed the urea-based counterpart (S1), suggesting a superior enhancement of antibacterial properties through diamide modification.

These findings highlight the potential of amide-functionalized carbon nanotube composites as promising antimicrobial agents and underscore the importance of chemical design in optimizing biological activity for future biomedical and environmental applications.

Funding

The authors declare that no funds, grants, or other support were received during the preparation of this manuscript.

Data availability

The authors confirm that the data supporting the outcomes of this research are accessible within the article

Acknowledgements

The authors would like to acknowledge Sulaimani University, College of Science, Chemistry department and Al-Iraqia University College of Education, for materials characterization, and laboratory Management, for research facilities and data analysis

Author Contributions

Material preparation, data collection and analysis were performed by [Kareem Jumaah Al-Salihi and Qadoori Zedan khalaf]. The Authors read and approved the final manuscript.

Conflict of interest

The authors have no relevant financial or non-financial interests to disclose.

Ethics approval and consent to participate

All the procedures followed were in accordance with ethical standards.

Consent for publication

Not applicable.

Research involving human participants and/or animals

Not applicable.

Informed consent

Not applicable.

References

[1] Sumio Iijima (1991) "Helical microtubules of graphitic carbon" *Nature*, **Vol. 354**, 56–58

[2] Dimitrios Tasis, Nikos Tagmatarchis. Alberto Bianco , Maurizio Prato (2006) "Chemistry of carbon nanotubes. *Chemical Reviews*, **Vol. 106 (3),** 1105–1136.

[3] Yi Lin, Shelby Taylor, Huaping Li, K. A. Shiral Fernando, Liangwei Qu, Wei Wang, Lingrong Gu, Bing Zhou and Ya-Ping Sun (2004) "Advances toward bio applications of carbon nanotubes" *J Mater Chem.,* **Vol. 14**, 527-541.

[4] Alberto Bianco , Kostas Kostarelos , Maurizio Prato. (2005). Applications of carbon nanotubes in drug delivery. *Current Opinion in Chemical Biology*, **Vol. 9(6),** 674–679.

[5] Alberto Bianco, Kostas Kostarelos, Charalambos D. Partidos and Maurizio Prato (2005) "Biomedical applications of functionalized carbon nanotubes" *Chem. Commun.,* 571–577.

[6] Rachel Yoon Kyung Chang, Sue C. Nang, Hak-Kim Chan, Jian Li (2022) "Novel antimicrobial agents for combating antibiotic-resistant bacteria" *Advanced Drug Delivery Reviews,* Vol. 187, 114378.

[7] Marta Roldo and Dimitrios G. Fatouros (2013)" Biomedical applications of carbon nanotubes" *Annu. Rep. Prog. Chem., Sect. C: Phys. Chem*., **109,** 10- 35.

[8] Qadoori Zedan Khalaf, Moneer K. Mohsen, Kareem Jumaah Jibrael Al-Salihi, Rebaz Anwar Omer, and Yousif Hussein Azeez, (2024)" Synthesis andDensity Functional Theory Study on the Functionalization of Carbon Nanotube Conjugates with Amino Compounds and Their Application in Dyeing Processes" *ChemistrySelect Vol.* **25,** *9*, e202403525 (1 of 10)

[9] Sandhya Vardharajula, Sk Z Ali, Pooja M Tiwari , Erdal Eroğlu , Komal Vig , Vida A Dennis , Shree R Singh (2012) " Functionalized carbon nanotubes: biomedical applications" *Int J Nanomedicine,* **Vol. 7**, 5361–5374. doi: 10.2147/IJN.S35832

[10] Alberto Bianco , Kostas Kostarelos , Maurizio Prato (2005) "Applications of carbon nanotubes in drug delivery" *Current Opinion in Chemical Biology*, **Vol.9**, 674-679

[11] Marisa Gomes, Rita Teixeira-Santos, Luciana C. Gomes, Francisca Sousa-Cardoso, Fábio M. Carvalho, Andreia R. Tomé, Olívia S. G. P. Soares, Kathryn A. Whitehead and Filipe J. Mergulhão (2023) "Antibiofilm Effect of Nitric Acid-Functionalized Carbon Nanotube-Based Surfaces against E. coli and S. aureus" *Antibiotics*, **12**, 1620 -1636.

[12] Seoktae Kang, Meagan S. Mauter , Menachem Elimelech (2008) 'Physicochemical determinants of multiwalled carbon nanotube bacterial cytotoxicity', *Environ. Sci. Technol*., **Vol. 42**, (19), pp. 7528–7534

[13] Massimiliano Olivi, Elena Zanni, Giovanni De Bellis,bh Claudio Talora, Maria Sabrina Sarto, Claudio Palleschi, Emmanuel Flahaut, Marc Monthioux, Stefania Rapino, Daniela Uccelletti and Silvana Fiorito, (2013) 'Inhibition of microbial growth by carbon nanotube networks', *Nanoscale*, **Vol. 5(19),** 9023–9029.

[14] Seoktae Kang , Meagan S. Mauter , Menachem Elimelech (2009) 'Microbial cytotoxicity of carbonbased nanomaterials: implications for river water and wastewater effluent', *Environ. Sci.Technol*., **Vol. 43**, pp. 2648–2653

[15] Karthika Prasad, G. S. Lekshmi, Kola Ostrikov, Vanessa Lussini, James Blinco, Mandhakini Mohandas, Krasimir Vasilev Steven Bottle , Kateryna Bazaka & Kostya Ostrikov (2017) 'Synergic bactericidal effects of reduced graphene oxide and silver nanoparticles against gram-positive and gram-negative bacteria', *Sci. Rep*.,**7**, 1591

[16] Haito Li, Xiaodie He, Yang Liu, Hui Huang, Suoyuan Lian, Shuit-Tong Lee (2011) 'One-step ultrasonic synthesis of water-soluble carbon nanoparticles with excellent photoluminescent properties', *Carbon.,* **49,** 605–609.

[17] Jau-Yi Wu, Ching-Wen Li, Ching-Hsiu Tsai, Chih-Wei Chou, Dar-Ren Chen and Gou-Jen Wang (2014) 'Synthesis of antibacterial TiO2/PLGA composite biofilms' *Nanomedicine: Nanotechnology, Biology and Medicine,* **Vol. 10, Issue 5** e1097-e1107.

[18] Ji, H., Sun, H., Qu, X. 'Antibacterial applications of graphene-based nanomaterials: recent achievements and challenges', *Adv. Drug Deliv. Rev.,* **Vol. 105**, 176–189

[19] Sahar E. Abo-Neima1 , Hussein A. Motaweh1 , Emad M. Elsehly (2020) "Antimicrobial activity of functionalized carbon nanotubes against pathogenic microorganisms" *IET Nanobiotechnol*., **Vol. 14(6),** 457-464.

[20] Khalid Saeed and Soo-Young Park (2010) "Preparation and characterization of multiwalled carbon nanotubes/polyacrylonitrile nanofibers" *J. Polym. Res.,* **Vol. 17,** 535–540 DOI 10.1007/s10965-009-9341-4

[21] Bauer, A.W.; Kirby, W.M.; Sherris, J.C.; Turck, M. (1966) "Antibiotic susceptibility testing by a standardized single disk method" *Am. J. Clin. Pathol.* **45,** 493–496.

[22] Zeeshan A. Khan, Mohd F. Siddiqui, and Seungkyung Park, (2019)" Current and Emerging Methods of Antibiotic Susceptibility Testing", *Diagnostics*, **Vol. 9**, 49.

[23] Marina Gonza´lez-Sa´nchez, Jorge S. Valera, Jacobo Veiga-Herrero, Paula B. Chamorro,a Fa´tima Aparicio and David Gonza´lez-Rodrı´guez , (2025) "Self-assembled nanotubes from the supramolecular polymerization of discrete cyclic entities" *Chem. Soc. Rev.,* **Vol. 54**, 5657–5697.

[24] Ana Maria Díez-Pascual, (2021) "Chemical Functionalization of Carbon Nanotubes with Polymers: A Brief Overview" *Macromol,* **Vol. 1**, 64–83. https://doi.org/10.3390/macromol1020006

[25] Rasel Das, Sharifah Bee Abd Hamida, Md. Eaqub Ali , Seeram Ramakrishna and Wu Yongzhi, (2015)" Carbon Nanotubes Characterization by X-ray Powder Diffraction – A Review" *Current Nanoscience*, **Vol. 11,** No. 1

[26] Oddershede, J.; Nielsen, K.; Stahl, K. (2007) "Using X-ray powder diffraction and principal component analysis to determine structural properties for bulk samples of multiwall carbon nanotubes" *Z. Kristallogr,* **Vol. 222,** 186-192.

[27] Robert Hammond, Klimentina Pencheva, Kevin J. Roberts, Patricia Mougin and Derek Wilkinson, (2005) "An examination of the thermal expansion of urea using high-resolution variable-temperature X-ray powder diffraction" *J. Appl. Cryst*. **Vol. 38,** 1038–1039

[28] Brandon C, Joshua H, Joe V, Williams S. (2012) "X-ray fluorescence as a method of monitoring metal catalyst content during the purification of carbon nanotubes" *Radiation Physics and Chemistry*. **Vol. 81(2),** 131-134

[29] García-Gutiérrez MC, Nogales A, Hernández JJ, Rueda DR, Ezquerra TA (2007) "X-ray scattering applied to the analysis of carbon nanotubes, polymers and nanocomposites" *Opt Pura Apl.,* **Vol. 40(2),** 195–205

[30] Kiran Sankar Maiti, (2018) " Ultrafast N–H vibrational dynamics of hydrogen-bonded cyclic amide reveal by 2DIR spectroscopy" *Chemical Physics*, **Vol. 515**, 509-512.

[31] Hossein Naeimi, Ali Mohajeri, Leila Moradi, and Ali Morad Rashidi, (2011) "Solubilization of Multi Walled Carbon Nanotubes Under a Facile and Mild Condition" Journal of *Nanoscience and Nanotechnology* **Vol. 11**, 1–4.

[32] Andrew T. Krasley, Eugene Li, Jesus M. Galeana, Chandima Bulumulla, Abraham G. Beyene, and Gozde S. Demirer, (2024) "Carbon Nanomaterial Fluorescent Probes and Their Biological Applications" *Chem. Rev.* **Vol. 124**, 3085−3185.

[33] Ashley D. Slattery, Cameron J. Shearer, Joseph G. Shapter, Adam J. Blanch, Jamie S. Quinton and Christopher T. Gibson, (2018) "Improved Application of Carbon Nanotube Atomic Force Microscopy Probes Using Peak Force Tapping Mode" *Nanomaterials*, **Vol. 8**, 807, doi:10.3390/nano8100807.

[34] Olga V. Zakharova, Alexander A. Gusev , Peter A. Baranchikov , Svetlana P. Chebotaryova, Svetlana S. Razlivalova, Elina Y. Koiava, Anna A. Kataranova, Gregory V. Grigoriev, Nataliya S. Strekalova and Konstantin V. Krutovsky, (2025) " The Composition of the Dispersion Medium Determines the Antibacterial Properties of Copper (II) Oxide Nanoparticles Against Escherichia coli Bacteria" *Nanomaterials*, **Vol. 15,** 469.